Oil Shale, 2026, 43, 1, 54–74 https://doi.org/10.3176/oil.2026.1.03

Major, trace, and rare earth elements geochemistry and enrichment in the Neogene organic-rich sediments from the Aleksinac deposit (Serbia): Part A

Gordana Gajica[(a)]*, Aleksandra Šajnović[(a)], Ksenija Stojanović[(b)], Milan D. Antonijević[(c)], Aleksandar Kostić[(d)], Branimir Jovančićević[(b)]

[(a)] Center of Chemistry – Institute of Chemistry, Technology and Metallurgy, University of Belgrade, Njegoševa 12, 11000 Belgrade, Serbia
[(b)] Faculty of Chemistry, University of Belgrade, Studentski trg 12-16, 11000 Belgrade, Serbia
[(c)] School of Chemistry and Chemical Engineering, University of Surrey, Guildford, Surrey GU2 7XH, United Kingdom
[(d)] Faculty of Mining and Geology, University of Belgrade, Đušina 7, 11000 Belgrade, Serbia

Received 30 April 2025, accepted 23 January 2026, available online 29 January 2026

Abstract. *The composition of inorganic matter and the enrichment of trace and rare earth elements (TEs and REEs) in the Neogene organic matter-rich sediments in the Upper layer of the Aleksinac deposit (Dubrava block, Serbia) were analysed. Correlation analysis clearly showed that TEs and REEs are associated with SiO_2, Al_2O_3, K_2O, and TiO_2, clastic minerals, clay, and feldspar, as well as zeolite minerals natrolite and analcime, indicating that the TEs and REEs were brought into the basin mainly by clastic material. Their distribution indicates certain changes in the depositional environment during the formation of these sediments. According to enrichment factors (calculated in relation to World Oil Shales, Upper Continental Crust, and Post-Archaean Australian Shale) and the degree of enrichment (relative to argillaceous rocks), the Aleksinac oil shale shows significant enrichment in Mo, a lesser degree in Sr, and possible enrichment in Cu. Therefore, there are no concerns regarding toxic trace elements in the Aleksinac oil shale.*

Keywords**:** *mineral composition, geochemical association of elements, enrichment factors, degree of enrichment.*

* Corresponding author, gordana.gajica@ihtm.bg.ac.rs

© 2026 Authors. This is an Open Access article distributed under the terms and conditions of the Creative Commons Attribution 4.0 International License CC BY 4.0 (http://creativecommons.org/licenses/by/4.0).

1. Introduction

Oil shales are the subject of numerous research activities due to their economic importance as a potential energy source and industrial raw material, since they represent an important reservoir of organic carbon and trace elements. The inorganic matter makes up the largest part of the oil shale, while the organic matter (OM) is dispersed within it, most often forming a homogeneous mixture. Generally, oil shales are characterised by fine lamination in which laminae of mixed organic and mineral matter, and pure mineral material alternate [1]. Oil shales vary in the content of the inorganic part, which commonly ranges from 60% to 90% [2].

As the prevalent part of oil shale comprises inorganic matter, the analysis of mineral and chemical composition (major, trace, and rare earth elements) is important for utilisation, economic-geological, environmental, and geochemical aspects. Oil shales enriched in certain elements can be used as a mineral raw material in metallurgy. From the economic-geological assessment of oil shale deposits, the content of certain individual elements (e.g. V, Zn, Cu, and U) may contribute to its greater value. On the other hand, during the exploitation and processing of oil shales, there is a possible mobilisation and concentration of elements, leading to their release into the water, air, and soil. This is undesirable from the aspect of environmental protection and can have a negative impact on the environment and health, especially if certain elements are present in high concentrations [3–9].

The trace and rare earth elements (TEs and REEs, respectively) are present in low concentrations in oil shale; they do not exist independently and can be found in the form of organometallic compounds, embedded in the crystal structure of minerals, or in a dispersed state on clay and oxyhydroxide particles [10]. It has been proven that oil shales can be enriched in certain TEs and REEs, as can other OM-rich sediments, e.g. coals [7, 11, 12]. Elevated concentrations of certain elements in oil shales can be determined by comparing their contents with some ‘standard values’. The most commonly used ‘standard values’ are the composition of the Upper Continental Crust (UCC) [13–18], Post-Archaean Australian Shale (PAAS) [13], North American Shale (NASC) [19–21], the average World Oil Shales (WOS) [22–26], and argillaceous rocks [26]. The TEs enrichment and geochemical investigation of OM-rich sediments also require an analysis of major element distribution, as these elements are diagenetically stable and can reflect the sedimentary background (terrigenous detrital influence) [27].

The Aleksinac oil shale deposit is the largest and richest oil shale deposit in Serbia and has significant economic importance [4, 28]. Therefore, it is the most investigated oil shale in Serbia, but studies on its inorganic composition are rare. The aims of this study were to determine: (i) the composition of inorganic matter; (ii) the geochemical association of elements; and (iii) the enrichment of TEs and REEs. Outcrop samples from the Upper layer of

the Dubrava block of the Aleksinac deposit were selected for this study. The study's findings may be useful for future exploration and utilisation of oil shales.

2. Samples and analytical methods

2.1. Samples and geological background

The Aleksinac deposit was formed within the Great Moravian–South Moravian Depression during the Neogene, within a lake basin that developed due to tectonic activities, climatic conditions, and the inflow of water and clastic material [28, 29]. According to some authors [29, 30], the area of the Aleksinac basin was located on two geotectonic units, the Carpatho-Balkanides and the Serbian–Macedonian Massif, and the lake sediments were deposited in tectonic depressions formed by the fragmentation of these two geotectonic units. The Aleksinac basin is filled with Lower and Upper Miocene lake sediments. However, oil shales were formed only during the Lower Miocene [3]. These sediments are characterised by the rhythmic appearance of different lithological units and oil shales, indicating frequent sedimentation changes [29]. The Lower Miocene sediments are of lacustrine origin: they start with red conglomerates, overlain by alluvial–lacustrine sandstones, with some sandy shale and siltstone in the upper layers. Above these sediments, two layers of oil shales (Lower and Upper) were deposited, with the Aleksinac Main coal seam located between them. A layer of Upper Miocene marl, clay, sand, and conglomerate unconformably covers the Lower Miocene complex. As a result of complex tectonic movements, the Aleksinac deposit is divided by fault zones into three main blocks from north to south: Dubrava, Morava, and Logorište [3, 30, 31]. According to certain characteristics of organic matter and mineral base, the Aleksinac deposit is closest to the Green River shale, in which the deposition of sedimentary rocks took place in a shallow reducing environment of a stratified, brackish–saline alkaline lake [3, 29].

For this study, sediment samples were taken from the Dubrava block, from the outcropping Upper oil shale layer. Sixteen samples (D1–D16) were collected as discontinuous channel samples comprising a 250 m thick series, from the top of the bituminous marl sequence to the bottom of the Upper oil shale layer, just above the Main coal seam. The Upper oil shale layer is much thicker and more accessible, and thus easier for exploitation and processing. A detailed description of the lithostratigraphic column of the analysed samples is provided in previous publications [32, 33].

Based on mineral composition, eight samples are defined as marlstones (D2, D3, D5, D8, D12–D15), five as mudstones (D1, D4, D6, D7, D9), two as calcareous mudstones (D10, D11), and one as calcareous marlstone (D16; Table 1) [33].

2.2. Analytical methods

2.2.1. Inductively coupled plasma optical emission spectroscopy

The content of major elements was determined by inductively coupled plasma optical emission spectroscopy (ICP-OES, Thermo iCAP 6500). Lithium metaborate ($LiBO_2$) fusion was used to prepare sample solutions for the analysis. The samples were mixed with $LiBO_2$ flux in graphite crucibles, and the crucibles were then fused in a furnace at 900 °C for 15 min. After cooling, the content from the crucibles was transferred into plastic bottles and dissolved with 150 cm^3 of 3.5% HNO_3. The samples were mixed using a magnetic stirrer for an hour, then filtered and dissolved with deionised water to a volume of 250.00 cm^3.

2.2.2. Inductively coupled plasma mass spectrometry

The content of 39 TEs and REEs was determined by inductively coupled plasma mass spectrometry (ICP-MS, Thermo X Series II ICP-MS). The samples were prepared in the same way as for ICP-OES analysis. From the obtained solution, 0.25 cm^3 was placed in a test tube and supplemented with an internal standard solution to a volume of 5.00 cm^3. The internal standard solution contained 1.05 cm^3 of Rh solution (concentration 10 ppm Rh in 3% HNO_3), 60 cm^3 of concentrated nitric acid, and deionised water to a total volume of 2000 cm^3. A rack of samples on both instruments (ICP-OES and ICP-MS) comprised, in addition to samples, three analytical blanks, one internal reference material (BEN), four certified reference materials (OU, SCO, ACE, and GCN), and two standards (QC1 and QC2), which enabled a quick check of analytical quality. Before analysing the prepared blanks, standards, and samples, a high-purity standard (SD12) was used for instrument calibration and stabilisation. ICP-OES and ICP-MS measurements were carried out in triplicate.

2.2.3. Rock-Eval pyrolysis, elemental analysis, and XRD analysis

The total organic carbon (TOC) content was determined by Rock-Eval pyrolysis using a Rock-Eval 6 Standard analyser. The content of total sulphur (TS) was measured with an elemental analyser (Vario EL III, CHNOS Elemental Analyser, Elementar Analysensysteme GmbH). The mineral composition was analysed with an XRD analyser (Bruker D8 Advance diffractometer). The semi-quantitative mineral composition was obtained using TOPAS Rietveld refinement software. Detailed procedures for these analyses are provided in a previous paper [33].

2.3. Data analysis and calculation

Cluster analysis was performed using SPSS 20 to group the samples based on similarities and differences. The same program was also used for the

correlation analysis of parameters, while Microsoft Excel 2013 and Origin 2016 were applied for correlation between a smaller number of elements and for graphical presentation. Principal component analysis (PCA) was performed in Minitab 17 to reduce the number of variables necessary to describe the dataset, to visualise the data structure, and to determine the association of elements more easily.

Due to the low concentrations of TEs and REEs, an enrichment factor (EF) is used to follow their distributions. The EF is used to describe the enrichment of an element in sedimentary rocks ($EF_{element\ X}$), calculated as the ratio of the concentration of an element (X) in the analysed sample to its content in certain 'standard samples'. To minimise the dilution effect of OM and authigenic minerals, element concentrations are normalised to Al, due to its resistance to alteration processes. If Al resides within the detrital clay fraction of the sediments (determined by the correlation of Al with Ti), it is appropriate to use Al content for normalisation [34, 35]:

$$EF_{element\ X} = (X/Al)_{sample}/(X/Al)_{standard}. \quad (1)$$

Furthermore, solid fossil fuels can be characterised based on the degree of enrichment with a certain element (Q_i) in relation to the concentration of that element (K1*i*) in argillaceous rocks (the most abundant sedimentary rock type, including oil shale) [25]:

$$Q_i = C_i/K_{1i}, \quad (2)$$

where C_i is the average concentration of the i^{th} element in the dry samples. According to Q_i values, caustobiolites (fossil combustible substances) are classified into five groups: (i) < 0.6 = noticeably depleted in TEs; (ii) 0.6–1.4 = differ little in the amount of TEs; (iii) 1.4–2.0 = enriched in TEs to a certain extent; (iv) 2.0–3.5 = noticeably enriched in TEs; and (v) > 3.5 = considerably enriched in TEs [25].

3. Results and discussion

3.1. Mineralogy and geochemistry of the investigated samples

3.1.1. Mineral composition

The semi-quantitative mineral composition of samples is presented in Figure 1. Samples D1–D15 have similar mineral compositions, while sample D16 notably differs.

Samples D1–D15 show variations in the concentrations of clays, feldspars, quartz, carbonates, analcime, and natrolite (Fig. 1). The elevated content of carbonate minerals distinguishes D2 and D13. The highest content of clay minerals is found in samples D1, D6, D7, D9, and D10. The highest amount of quartz is observed in samples D2, D5, and D13; it is present in a very low

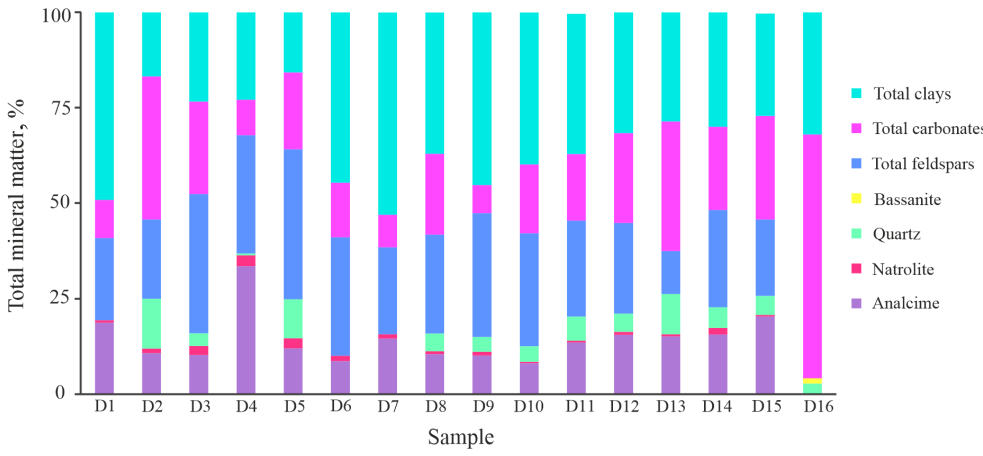

Fig. 1. Semi-quantitative mineral composition.

amount (0.48 wt%) in sample D4, while quartz is absent in samples D1, D6, and D7. The highest content of feldspar minerals characterises samples D3–D6 and D9. An elevated content of analcime is found in sample D4, followed by samples D1 and D15. The highest content of natrolite is present in samples D3–D5.

The uniqueness of sample D16 is reflected in its significantly higher content of authigenic carbonate minerals (accounting for 63.87 wt% of the total mineral matter), the absence of terrigenous detrital minerals (feldspars) and zeolite minerals (analcime and natrolite), and the presence of the sulphate mineral bassanite, which is identified only in this sample.

3.1.2. Major elements

The contents of major elements in the analysed samples, together with TOC and TS, are listed in Table 1.

Among the major elements, SiO_2, Al_2O_3, Fe_2O_3, and CaO are the most abundant, whereas TiO_2, MnO, and P_2O_5 are the least abundant (concentration <1 wt%; Table 1). SiO_2 and Al_2O_3 prevail in samples D1–D15, while CaO dominates in sample D16. This is consistent with the mineral composition of the analysed samples (Fig. 1). Samples D1–D15 are characterised by increased content of constituents of clastic minerals SiO_2, Al_2O_3, K_2O, and TiO_2, followed by Fe_2O_3. Al_2O_3 and SiO_2 are most abundant in clay minerals and quartz (SiO_2). In contrast, sample D16 is characterised by the prevalence of CaO, which is in accordance with the dominance of carbonate minerals (Fig. 1; Table 1). Furthermore, sample D16 has a lower content of all other major elements. The elevated content of MgO in samples D1–D15 compared to D16 (Fig. 1; Table 1) can be explained by the presence of dolomite in all samples except D16 [33].

Table 1. Lithology, total organic carbon, total sulphur, and major elements, wt%

Sample	Lithology	TOC	TS	Al_2O_3	SiO_2	TiO_2	Fe_2O_3	K_2O	Na_2O	MgO	CaO	MnO	P_2O_5
D1	Mdst	2.85	0.13	17.85	42.98	0.76	8.35	3.27	3.69	3.42	5.35	0.10	0.40
D2	Mrl	7.06	0.21	9.09	31.99	0.45	4.90	2.10	1.69	7.80	13.08	0.12	0.15
D3	Mrl	3.87	0.18	13.23	36.32	0.66	7.57	3.41	1.63	6.12	9.89	0.11	0.12
D4	Mdst	1.79	0.13	17.93	44.57	0.77	9.67	3.18	4.28	2.53	4.26	0.11	0.27
D5	Mrl	5.44	0.23	13.63	42.27	0.62	5.24	3.68	1.45	4.66	8.08	0.08	0.06
D6	Mdst	1.31	0.13	17.50	43.99	0.87	7.13	4.36	2.10	3.63	7.36	0.12	0.17
D7	Mdst	1.88	0.13	17.31	45.30	0.79	8.83	3.31	3.17	3.56	4.76	0.11	0.20
D8	Mrl	5.20	0.15	12.97	38.11	0.62	6.16	3.44	2.08	4.43	10.78	0.11	0.14
D9	Mdst	5.10	0.09	16.05	45.45	0.75	7.90	3.79	2.13	4.48	4.20	0.10	0.05
D10	CalcMdst	8.22	0.08	13.08	34.91	0.67	6.75	3.07	1.69	4.77	7.70	0.10	0.43
D11	CalcMdst	3.83	0.07	14.02	40.95	0.63	8.23	3.35	2.14	4.99	7.37	0.09	0.04
D12	Mrl	7.20	0.08	12.30	36.07	0.59	6.23	2.82	2.17	5.01	9.99	0.11	0.09
D13	Mrl	13.10	0.21	8.67	29.93	0.43	4.62	1.76	2.02	6.87	10.92	0.08	0.06
D14	Mrl	4.01	0.06	13.05	39.00	0.64	7.50	2.98	1.94	7.52	8.32	0.11	0.05
D15	Mrl	8.61	0.14	11.76	33.48	0.57	6.53	2.77	2.61	5.81	10.20	0.10	0.19
D16	CalcMrl	29.10	6.11	5.13	17.74	0.15	2.54	1.08	0.25	1.63	36.13	0.04	0.05

Abbreviations: Mdst – mudstone; Mrl – marlstone; CalcMdst – calcareous mudstone; CalcMrl – calcareous marlstone.

Samples D1, D4, D6, D7, and D9 show the highest content of clastic mineral constituents such as Al_2O_3, SiO_2, and TiO_2 [36–38]. Some of these samples (D4, D6, D7) have the lowest TOC, probably due to the dilution effect of OM with clastic material (Table 1). The highest TOC content characterises sample D16, while samples D2, D10, D12, D13, and D15 also have relatively high TOC.

On the basis of the major element contents, the same conclusion can be drawn as from the mineral composition: there was a significant change in the diagenetic environment after the deposition of the sediments represented by sample D16, and also certain less pronounced variations during the formation of the sediments represented by samples D15–D1.

3.1.3. Trace elements

The contents of TEs in the analysed samples are listed in Table 2. Based on TE contents, sample D16 again differs significantly from samples D1–D15 (Table 2). Sample D16 is characterised by lower concentrations of almost all analysed TEs, while only Cs, Sr, Cr, and Ni are found in higher concentrations compared to samples D1–D15 (Table 2).

The obtained result can be attributed to changes in the origin of sedimentary material and/or depositional conditions after the sediment deposition represented by sample D16 (see Sections 3.1.1 and 3.1.2) [33]. Moreover, this sample originated from the oil shale layer just above the Main coal seam. In sedimentological terms, this shift indicates a change in the depositional environment, since different conditions are necessary for their formation, probably reflecting a transition from a wetland to a lacustrine environment.

The variations in analysed TE concentrations among samples D1–D15 indicate certain changes in the depositional environment during sediment formation. Within this group, samples D1, D4, D6, and D7 stand out due to their elevated concentrations of most analysed TEs. In contrast, samples D2 and D13 are characterised by the lowest TE concentrations. This pattern is more visible on the dendrogram, which shows that the analysed samples are divided into two main clusters: D1–D15 (I) and D16 (II; Fig. 2a).

Samples D1–D15 are further divided into two subclusters. The first subcluster (Ia) includes samples D3, D5, D8, D10–D12, D14, and D15, as well as samples D2 and D13, which show slight separation, more pronounced in sample D13. The second subcluster (Ib) comprises samples D1, D4, D6, D7, and D9. The results are almost identical whether the cluster analysis is conducted based only on TE contents (Fig. 2a) or using the contents of major, trace, and rare earth elements, total organic carbon, and total sulphur (Fig. 2b).

Table 2. Contents of trace elements, ppm

Element	D1	D2	D3	D4	D5	D6	D7	D8	D9	D10	D11	D12	D13	D14	D15	D16
Rb	107.15	74.71	109.65	89.14	118.05	120.25	102.55	104.05	134.45	102.95	121.95	91.65	70.82	127.45	90.35	68.56
Cs	8.60	5.75	7.45	9.69	7.95	8.26	8.72	7.07	9.32	7.91	9.32	6.49	4.84	8.94	6.20	41.55
Be	2.31	1.30	2.04	2.45	1.71	2.25	2.25	1.91	2.28	2.03	1.96	1.65	1.19	1.93	1.63	0.66
Sr	297.00	743.00	581.00	260.00	469.00	444.00	365.00	585.00	256.00	470.00	458.00	504.00	644.00	480.00	532.00	1592.00
Ba	473.67	391.05	490.85	512.30	412.10	592.64	536.33	437.62	425.90	481.22	406.74	427.79	381.51	435.34	420.84	339.91
Sc	12.94	11.02	17.48	26.58	9.86	16.01	16.12	13.71	15.73	15.84	13.17	12.95	11.73	16.64	13.74	5.70
Zr	47.78	31.34	40.29	44.31	41.46	74.79	51.72	59.29	47.08	43.02	46.78	39.71	30.11	46.48	38.07	21.30
Hf	1.36	1.08	1.35	1.38	1.36	2.26	1.54	1.90	1.75	1.31	1.32	1.30	0.95	1.63	1.20	0.78
V	156.00	98.00	145.00	217.00	129.00	117.00	183.00	135.00	187.00	144.00	149.00	134.00	104.00	174.00	142.00	55.00
Nb	9.92	5.95	8.59	9.73	8.46	11.03	9.94	8.22	9.48	8.77	8.41	7.80	5.70	8.60	7.48	3.24
Ta	0.71	0.42	0.62	0.72	0.61	0.80	0.73	0.64	0.70	0.62	0.60	0.57	0.41	0.62	0.53	0.23
Cr	92.23	53.66	82.06	99.85	75.69	91.42	92.83	74.77	93.17	79.61	85.81	76.72	57.73	84.94	74.18	179.64
Mo	56.67	4.85	10.96	18.65	12.81	7.12	19.64	5.18	10.93	6.34	26.71	8.32	22.81	12.82	12.21	1.48
W	2.77	0.91	1.52	2.10	0.43	1.74	2.44	0.79	1.66	1.03	0.67	0.83	0.38	1.20	0.68	1.47
Co	22.34	13.03	19.91	18.07	16.22	16.21	20.25	16.69	20.47	13.94	22.94	19.86	14.12	23.42	20.70	19.83
Ni	51.27	27.50	45.52	33.11	42.35	35.85	48.43	38.75	50.49	39.88	54.17	46.85	35.77	49.04	40.25	372.09
Cu	112.34	60.58	82.52	136.17	77.30	76.49	107.10	57.71	112.64	79.38	98.72	86.41	53.90	86.36	70.51	21.59
Zn	141.00	57.00	92.00	110.00	85.00	91.00	131.00	89.00	112.00	96.00	104.00	83.00	75.00	103.00	91.00	30.00
Ga	24.25	12.55	18.43	24.07	18.72	23.40	23.00	17.68	21.63	18.53	18.95	16.78	12.10	18.48	16.56	5.94
Tl	0.56	0.28	0.41	0.48	0.37	0.59	0.57	0.39	0.46	0.36	0.45	0.33	0.23	0.40	0.33	0.27
Sn	2.81	1.39	2.15	2.82	2.66	2.77	2.76	2.07	2.50	2.17	2.48	1.88	1.35	2.21	2.12	0.72
Pb	29.78	12.07	21.82	44.05	16.61	27.57	34.98	14.83	21.43	14.60	20.14	17.62	7.62	14.91	13.79	2.65
Th	12.46	8.50	10.54	18.26	6.87	12.42	14.99	11.03	6.55	16.39	3.30	8.20	8.57	4.77	10.12	3.22
U	10.66	5.59	3.62	7.54	1.95	4.07	4.74	3.54	2.36	6.83	1.57	2.43	2.36	1.64	6.04	1.75
Y	24.99	16.29	20.28	34.12	11.99	25.74	26.62	20.00	16.28	28.39	10.95	16.49	15.12	12.02	18.61	7.27

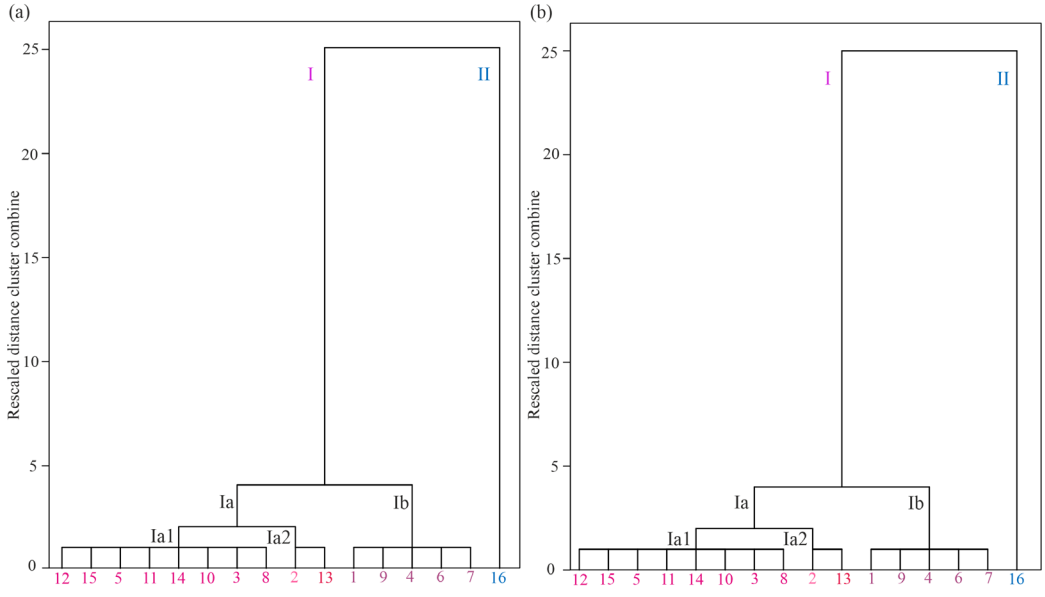

Fig. 2. Dendrograms of the studied samples derived from cluster analysis: (a) contents of trace elements and (b) contents of major, trace, and rare earth elements, total organic carbon, and total sulphur.

3.1.4. Rare earth elements

The contents of REEs in the analysed samples are listed in Table 3. REEs are present at lower concentrations in sample D16 compared to samples D1–D15 (Table 3; Fig. 3). Differences among samples D1–D15 can also be observed. Samples D4, D6, and D7, followed by sample D1, have higher concentrations of REEs, whereas samples D2, D5, D11, D13, and D14 contain lower amounts. Furthermore, sample D4 shows elevated concentrations of all REEs except Yb, which has the highest concentration in sample D1. Since samples D4, D6, and D7 are characterised by relatively high contents of clastic constituents (see Sections 3.1.1 and 3.1.2), it can be assumed that the REEs were probably delivered into the depositional environment with clastic material.

Generally, in the analysed samples, light earth elements (LREEs) are more abundant than heavy rare earth elements (HREEs; Table 3), which is in agreement with the typical distribution of REEs in oil shale [20, 37–40]. Based on PAAS-normalised REEs curves [13], it is also evident that sample D16 is clearly distinguished, as are samples D4, D6, and D7 (Fig. 3). The samples show no strong Ce anomalies, whereas several samples display negative Eu anomalies (D2–D4, D9, D11, D12, D14; Fig. 3).

Table 3. Contents of rare earth elements, ppm

Element	D1	D2	D3	D4	D5	D6	D7	D8	D9	D10	D11	D12	D13	D14	D15	D16
La	28.71	19.80	27.45	37.36	22.02	33.54	35.73	27.22	25.09	24.84	17.37	25.98	20.40	20.88	24.92	10.60
Ce	51.95	35.44	51.78	73.98	40.62	70.89	66.75	49.23	44.09	48.43	34.44	48.15	35.25	35.89	45.23	16.59
Pr	6.52	4.43	6.40	9.03	4.77	8.31	8.49	5.98	5.51	6.07	4.29	5.92	4.41	4.35	5.55	1.91
Nd	24.73	16.72	24.14	34.56	17.93	32.27	32.27	22.60	20.64	23.92	16.18	22.65	17.45	16.32	21.08	6.98
Sm	5.14	3.49	5.13	7.38	3.59	6.81	6.69	4.69	4.14	5.21	3.06	4.43	3.60	3.27	4.36	1.46
Eu	1.04	0.69	1.00	1.48	0.71	1.35	1.33	0.95	0.80	1.11	0.58	0.89	0.75	0.63	0.89	0.34
Gd	4.42	3.10	4.35	6.59	3.02	5.78	5.79	4.21	3.55	5.02	2.50	3.99	3.31	2.82	3.93	1.30
Tb	0.76	0.50	0.73	1.13	0.47	0.96	0.94	0.70	0.59	0.89	0.40	0.65	0.57	0.45	0.65	0.21
Dy	4.64	2.99	4.08	6.57	2.58	5.42	5.47	3.96	3.32	5.44	2.20	3.55	3.20	2.46	3.68	1.22
Ho	0.95	0.63	0.80	1.34	0.48	1.00	1.03	0.79	0.63	1.11	0.45	0.66	0.61	0.48	0.71	0.25
Er	3.09	1.94	2.24	3.92	1.29	2.81	2.87	2.22	1.74	3.13	1.29	1.76	1.61	1.36	2.08	0.73
Tm	0.49	0.30	0.32	0.54	0.18	0.38	0.39	0.33	0.24	0.46	0.19	0.23	0.21	0.20	0.30	0.10
Yb	3.66	2.00	1.98	3.17	1.18	2.40	2.38	2.07	1.57	3.12	1.26	1.44	1.29	1.35	1.89	0.71
Lu	0.56	0.29	0.29	0.44	0.18	0.35	0.34	0.33	0.23	0.44	0.19	0.22	0.19	0.20	0.27	0.10
LREEs	118.09	80.57	115.9	163.79	89.64	153.17	151.26	110.67	100.27	109.58	75.92	108.02	81.86	81.34	102.03	37.88
HREEs	18.57	11.75	14.79	23.70	9.38	19.10	19.21	14.61	11.87	19.61	8.48	12.50	10.99	9.32	13.51	4.62
∑REEs	136.66	92.32	130.69	187.49	99.02	172.27	170.47	125.28	112.14	129.19	84.40	120.52	92.85	90.66	115.54	42.50

Light rare earth elements (LREEs) = (La + Ce + Pr + Nd + Sm + Eu); heavy rare earth elements (HREEs) = (Gd + Tb + Dy + Ho + Er + Tm + Yb + Lu); ∑REEs = LREEs + HREEs.

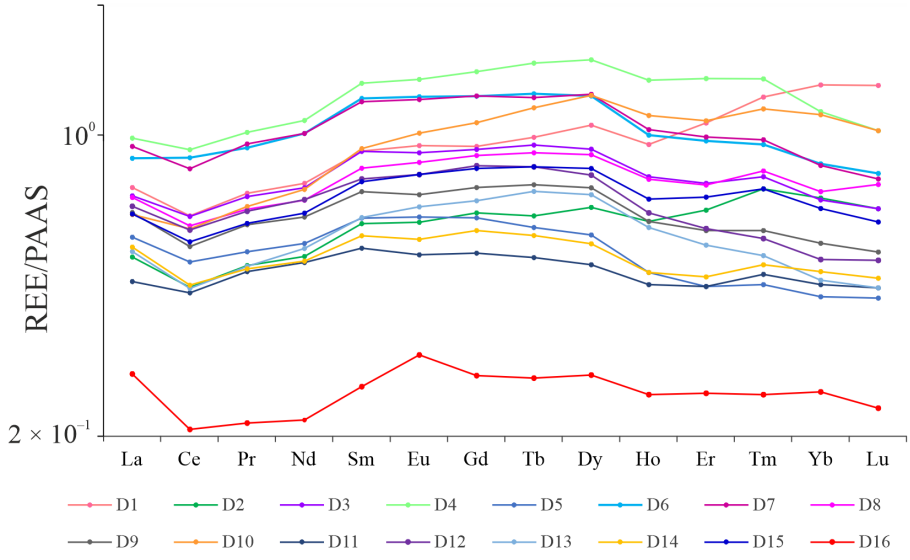

Fig. 3. Distribution of rare earth elements.

3.2. Geochemical association of trace and rare earth elements

The organic and inorganic matter of oil shale may host sedimentary accumulations of TEs and REEs. Their correlations with OM (i.e. TOC content) and the contents of inorganic components were performed for samples D1–D15, which originated from the same facies.

Regarding the OM, the correlation analysis shows that almost all TEs and REEs exhibit statistically significant negative correlations with TOC. A statistically significant positive correlation with TOC is observed for Sr only (at a significance level $p < 0.05$), whereas Cs, Be, Ba, Zr, Nb, Ta, Cr, W, Cu, Ga, Tl, Sn, and Pb ($p < 0.01$); Rb, Hf, V, and Zn ($p < 0.05$) from TEs; and La, Ce, Pr, Nd, and Sm ($p < 0.05$) from REEs showed significant negative correlations with TOC. This leads to the assumption that TEs are not associated with the OM of the examined sediments.

Statistically significant positive correlations with TOC are observed for major elements CaO and MgO ($p < 0.05$), as well as for carbonates and quartz ($p < 0.01$), whereas SiO_2, Al_2O_3, K_2O, TiO_2, and Fe_2O_3 exhibited negative correlations ($p < 0.01$). Considering that carbonate minerals have an authigenic origin, while quartz can have both authigenic and detrital origins, these correlations could imply that part of the quartz in the investigated samples has an authigenic origin [41, 42].

This is clearly evident in the loading plot obtained from the PCA (Fig. 4). The PCA resulted in a two-component model explaining 44.44% of the total

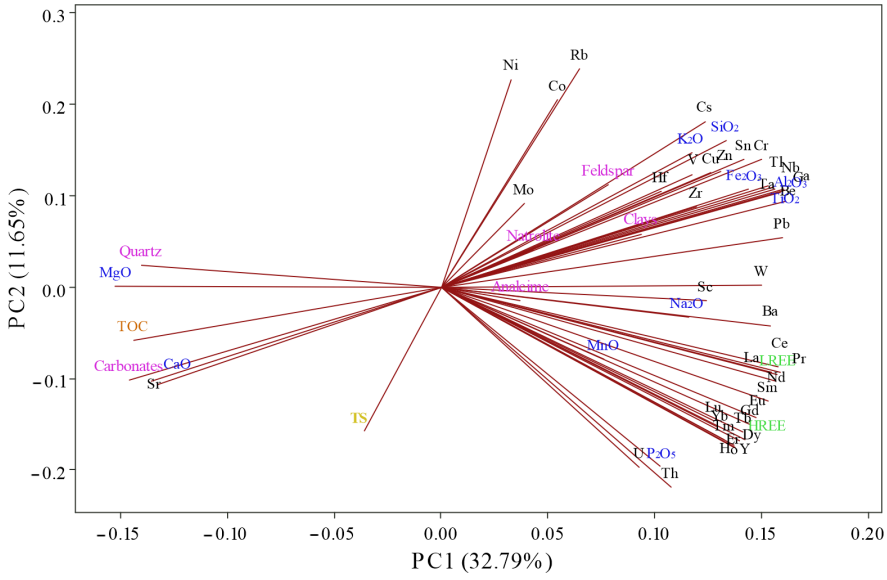

Fig. 4. Loading plot based on principal component analysis of minerals, major, trace and rare earth elements, TOC, and TS composition.

variance in the investigated dataset (minerals, major, trace, and rare earth elements, TOC, TS). The first principal component (PC1) accounted for 32.79% of the overall data variance, whereas the second (PC2) accounted for 11.65%.

Regarding the inorganic part, most of the examined TEs show statistically significant positive correlations with constituents of clastic minerals (SiO_2, Al_2O_3, K_2O, and TiO_2), clastic minerals (clay and feldspar), the zeolite mineral natrolite, and some TEs with analcime. On the other hand, negative correlations are observed between TEs and TOC, CaO, MgO, carbonate minerals, and quartz (Fig. 4). This confirms that TEs were brought into the basin mainly by clastic material, as expected.

The concentration of REEs shows statistically significant positive correlations with constituents of clastic minerals (Al_2O_3, TiO_2, SiO_2), followed by P_2O_5, Fe_2O_3, and Na_2O, but negative correlations with TOC, CaO and MgO, carbonate minerals, and quartz. Furthermore, LREEs and HREEs exhibit some differences in correlations. Namely, LREEs and HREEs show different significance of positive correlations with Na_2O: the LREEs demonstrate a positive correlation with SiO_2 ($p < 0.05$) and TiO_2 ($p < 0.01$), whereas the HREEs display a positive correlation with P_2O_5 ($p < 0.01$) and TiO_2 ($p < 0.05$; Fig. 4). Positive correlations of U and Th with P_2O_5 might indicate the presence of phosphate minerals monazite, xenotime, and apatite, together with heavy minerals (ilmenite, leucoxene, rutile, zircon) [43]. It is known that these minerals can be the source of REEs, as well as U and Th [44, 45]. Since XRD

analysis is not sensitive to less than 5 wt% of the crystalline phase present in the sample, it can be presumed that this technique did not identify the minerals mentioned above due to their low content.

3.3. Trace and rare earth elements enrichment

The average trace element concentrations of the analysed oil shales (AOS), the average World Oil Shales (WOSsp [25], WOSw [21, 22]), Upper Continental Crust (UCC, [12, 13, 16]), Post-Archaean Australian Shale (PAAS, [12]), and argillaceous rocks (K1i, [25]) are presented in Table 4. The enrichment factor (EF) and the degree of enrichment (Qi) are used to assess elemental enrichment in sedimentary rocks. The calculated EF and Qi of the analysed elements in the Aleksinac oil shales are given in Table 4. Furthermore, the range of element concentrations in oil shale ash from different deposits in Jordan (JOSa; Attarat Umm Al-Ghudran, El-Lajjun, Sultani, Jurf Al-Drawaish, Assfar Al-Mahata, Wadi Abu-Hmam, and Al-Shalaleh, [46]) are also presented in Table 4.

Based on the EF, meaningful enrichment of an element starts from values >3 [10], while if $EF > 1$, it can be only considered as a detectable enrichment [47]. In the analysed sample set for TEs, $EF > 3$ is found for Mo (in relation to WOSsp*, WOSw, UCC, PAAS), Sr (PAAS), and Cu (UCC; Table 4; Fig. 5). Therefore, it can be said that Mo shows significant enrichment, Sr to a lesser degree, and Cu to a possible degree.

Among REEs, some elements (Pr, Sm, Eu, Tb, Ho, Tm, Lu) show enrichment with respect to WOSw (Table 4; Fig. 5). The total average concentration of REEs in AOS is 118.88 ppm, which is lower than in WOSw (216.80 ppm), [21, 22], UCC (146.37 ppm) [12, 13, 16], and PAAS (183 ppm) [12]. The degree

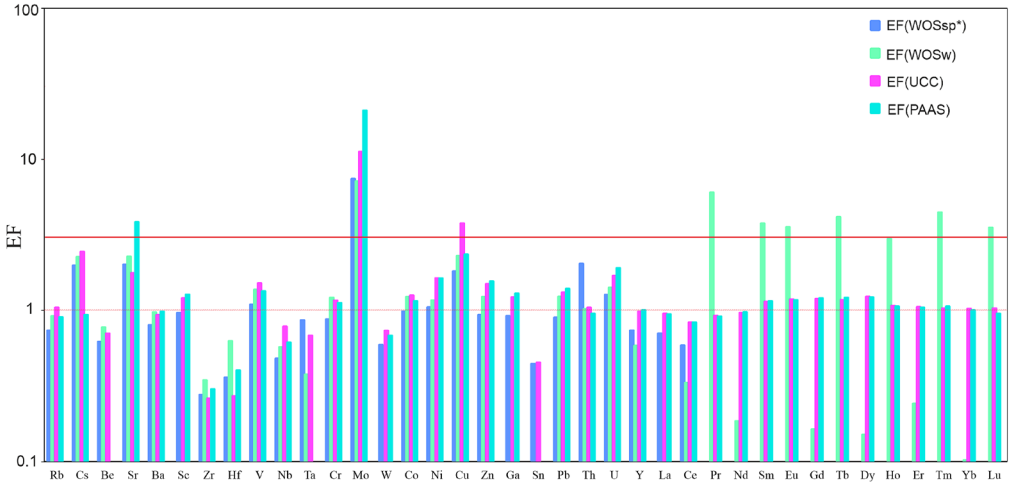

Fig. 5. Enrichment factors.

Table 4. Mean values of trace element concentrations in analysed oil shales (AOS), World Oil Shales (WOS), Upper Continental Crust (UCC), Post-Archaean Australian Shale (PAAS) and argillaceous rocks (K1i), enrichment factors (EFs), and degree of enrichment (Qi); range of concentrations in oil shale ashes from Jordan (JOSa)

TEs	AOS	WOSsp	WOSw	UCC	PAAS	K1i	EF(WOSsp*)	EF(WOSw)	EF(UCC)	EF(PAAS)	*Qi*	JOSa
Rb	102.11	139.1	140	112	160	130	0.73	0.91	1.04	0.90	0.79	-
Cs	9.88	5	5.5	4.60	15	2	1.98	2.25	2.44	0.93	4.94	-
Be	1.85	3	3	3	-	3	0.62	0.77	0.70	/	0.62	0.06–0.43
Sr	542.50	270	300	350	200	450	2.01	2.26	1.76	3.84	1.21	-
Ba	447.86	560	580	550	650	800	0.80	0.97	0.93	0.98	0.56	-
Sc	14.33	15	13	13.60	16	10	0.96	/	1.20	1.27	1.43	0.28–2.6
Zr	43.97	160	160	190	210	200	0.27	0.34	0.26	0.30	0.22	-
Hf	1.40	3.9	2.8	5.80	5	3	0.36	0.63	0.27	0.40	0.47	-
V	141.81	130	130	107	150	130	1.09	1.36	1.51	1.34	1.09	35.45–16 178
Nb	8.21	17.2	18	12	19	11	0.48	0.57	0.78	0.61	0.75	-
Ta	0.60	0.7	2	1	-	-	0.86	0.38	0.68	/	/	-
Cr	87.14	100	90	85	110	100	0.87	1.21	1.16	1.12	0.87	10.90–163.76
Mo	14.84	2	2.6	1.50	1	2	7.42	7.14	11.24	21.01	7.42	-
W	1.29	2.2	1.8	2	2.70	1.8	0.59	/	0.73	0.68	0.72	-
Co	18.63	19	19	17	23	19	0.98	1.23	1.25	1.15	0.98	0.23–1.52
Ni	63.21	60.5	68	44	55	95	1.04	1.16	1.63	1.63	0.67	7.20–73.05
Cu	82.48	45.6	45	25	50	57	1.81	2.29	3.75	2.34	1.45	3.30–28.09
Zn	93.13	100	95	71	85	80	0.93	1.23	1.49	1.55	1.16	-
Ga	18.19	20	19	17	20	20	0.91	/	1.22	1.29	0.91	-

Continued on the next page

Table 4. *Continued*

TEs	AOS	WOSsp	WOSw	UCC	PAAS	K1i	EF(WOSsp*)	EF(WOSw)	EF(UCC)	EF(PAAS)	Qi	JOSa
Sn	2.18	5	6	5.5	-	10	0.44	/	0.45	/	0.22	-
Pb	19.65	22	20	17	20	20	0.89	1.23	1.31	1.39	0.98	-
Th	9.76	4.8	12	10.70	14.60	12	2.03	1.02	1.04	0.95	0.81	-
U	4.17	3.3	3.7	2.80	3.10	3.7	1.26	1.41	1.69	1.90	1.13	-
Y	19.07	26	41	22	27	26	0.73	0.58	0.98	1.00	0.73	1.8–39.7
La	25.12	36	40	30	38	90	0.70	0.00	0.95	0.94	0.28	1.55–27.4
Ce	46.79	80	95	64	80	50	0.58	0.33	0.83	0.83	0.94	1.8–15.7
Pr	5.75	-	9.7	7.10	8.90	7.1	/	6.03	0.92	0.91	0.81	0.3–3.8
Nd	21.90	-	39	26	32	26	/	0.18	0.96	0.97	0.84	1.26–40.3
Sm	4.53	-	7.3	4.50	5.60	4.5	/	3.75	1.14	1.15	1.01	0.25–4.1
Eu	0.91	-	1.6	0.88	1.10	0.95	/	3.54	1.18	1.17	0.96	0.15–0.6
Gd	3.98	-	7	3.80	4.70	3.8	/	0.16	1.19	1.20	1.05	0.26–2.9
Tb	0.66	-	1.2	0.64	0.77	-	/	4.15	1.17	1.21	/	0.04–0.6
Dy	3.80	-	5.5	3.50	4.40	-	/	0.15	1.23	1.22	/	0.12–2.0
Ho	0.75	-	1.6	0.80	1.00	-	/	2.97	1.07	1.06	/	0.05–0.6
Er	2.13	-	3.9	2.30	2.90	-	/	0.24	1.05	1.04	/	0.14–2.2
Tm	0.30	-	0.6	0.33	0.40	-	/	4.44	1.03	1.06	/	0.02–2.6
Yb	1.97	-	3.7	2.20	2.80	2.2	/	0.10	1.02	1.00	0.89	0.12–2.7
Lu	0.29	-	0.7	0.32	0.43	-	/	3.52	1.03	0.95	/	0.02–0.6
∑REEs	118.88	-	216.8	146.37	183	-	/	/	/	/	/	8.72–148.31

- – not determined; / – cannot be calculated; the enrichment factors EF(WOSw), EF(UCC) and EF(PAAS) were calculated using the content of aluminium (Section 2.3), since for these sediments Al content (16.7%, 15.17%, 18.90%, respectively) was available, whereas for EF(WOSsp*) it was not available.

of enrichment for the investigated TEs was also determined based on Qi values (Table 4). Results suggest that the analysed oil shales are noticeably enriched in Mo and Cs and belong to the fifth group according to the classification proposed by Shpirt and Punanova [25]. Furthermore, they are enriched to a certain extent with Cu, U, and Sc, belonging to the third group, while analysed samples are noticeably depleted in Ba, Zr, Hf, Sn, La, and Yb and belong to the first group. The remaining TEs are in the second group, which indicates that the examined oil shales and argillaceous rocks differ slightly in the concentrations of these TEs.

Comparing the range of concentrations in oil shale ash from different deposits in Jordan with values in the analysed samples, it is notable that most elements fall within the range, while the following elements show higher concentrations in the analysed samples: Be, Sc, Co, Cu, Ce, Pr, Sm, Eu, Gd, Tb, Dy, and Ho [46].

4. Conclusions

The detailed inorganic geochemical characterisation of the Upper layer of Aleksinac oil shale in the Dubrava block was performed. The cluster analysis of major, trace, and rare earth elements, total organic carbon, and total sulphur showed that the analysed samples are divided into two main clusters, indicating certain changes in the depositional environment during the formation of these sediments.

Correlation analysis clearly showed that TEs and REEs are associated with SiO_2, Al_2O_3, K_2O, and TiO_2, clastic minerals, clay, and feldspar, as well as zeolite minerals natrolite and analcime, indicating that TEs and REEs were brought into the basin mainly by clastic material. Taking into account both the enrichment factors (calculated in relation to World Oil Shales, Upper Continental Crust, and Post-Archaean Australian Shale) and the degree of enrichment (concerning argillaceous rocks), it can be concluded that the Aleksinac oil shale is slightly enriched only in Cu, Cs, Sr, V, Ni, Zn, Pb, and U, whereas more significant enrichment is observed for Mo exclusively. The mentioned elements, except Cs, Sr, and Pb, are redox-sensitive, and therefore their enrichment is in accordance with the OM-richness of the studied samples.

Compared with ‘standard values’, there is no significant enrichment of elements potentially toxic to the environment and health in the analysed sediments, except for Mo and Cu. Therefore, there is a low risk of trace element pollution if the Aleksinac oil shale were to be further exploited.

Data availability statement

The data supporting the findings of this study are available within the article.

Acknowledgements

The study was financed by the Ministry of Education, Science and Technological Development of the Republic of Serbia (contract No. 451-03-136/2025-03/200168, project No. 451-03-136/2025-03/200026). We dedicate this paper to the memory of our colleague, Prof. Dr Aleksandar Kostić, who passed away during the preparation of this manuscript. The publication costs of this article were partially covered by the Estonian Academy of Sciences.

References

1. Tissot, B. P., Welte, D. H. *Petroleum Formation and Occurrence*. 2nd ed. Springer-Verlag, Heidelberg, 1984.
2. Dyni, J. R. *Geology and Resources of Some World Oil Shale Deposits*. U.S. Geological Survey Scientific Investigations Report 2005–5295, Reston, 2006.
3. Ercegovac, M. *Geologija uljnih škriljaca (Geology of Oil Shales)*. Građevinska knjiga, Beograd, 1990.
4. Ercegovac, M., Grgurović, D., Bajc, S., Vitorović, D. Oil shale in Serbia: geological and chemical-technological investigations, actual problems of exploration and feasibility studies. In *Mineral Material Complex of Serbia and Montenegro at the Crossings of Two Millenniums* (Vujić, S., ed.). Margo-Art, Belgrade, 2003, 368–378.
5. Song, D. Y., Ma, Y. J., Qin, Y., Wang, W. F., Zheng, C. G. Volatility and mobility of some trace elements in coal from Shizuishan Power Plant. *Journal of Fuel Chemistry and Technology*, 2011, **39**(5), 328–332. https://doi.org/10.1016/S1872-5813(11)60024-8
6. Fu, X., Wang, J., Zeng, Y., Tan, F., Feng, X. Concentration and mode of occurrence of trace elements in marine oil shale from the Bilong Co area, northern Tibet, China. *International Journal of Coal Geology*, 2011, **85**(1), 112–122. https://doi.org/10.1016/J.COAL.2010.10.004
7. Fu, X., Wang, J., Zeng, Y., Tan, F., Feng, X. Trace elements and their behaviour during the combustion of marine oil shale from Changliang Mountain, northern Tibet, China. *Environmental Earth Sciences*, 2012, **70**, 1125–1134. https://doi.org/10.1007/s12665-012-2199-5
8. Vallner, L., Gavrilova, O., Vilu, R. Environmental risks and problems of the optimal management of an oil shale semi-coke and ash landfill in Kohtla-Järve, Estonia. *Science of The Total Environment*, 2015, **524–525**, 400–415. https://doi.org/10.1016/j.scitotenv.2015.03.130
9. Han, Y. W, Ma, Z. D., Zhang, H. F., Zhang, B. R., Li, F. L., Gao, S. et al. *Geochemistry*. Geological Publishing House, Beijing, 2003.
10. Gluskoter, H. J., Ruch, R. R., Miller, W. G., Cahill, R. A., Dreher, G. B., Kuhn, J. K. *Trace Elements in Coal: Occurrence and Distribution*. Illinois State Geological Survey, Circular 499, Urbana, 1977.

11. Fu, X., Wang, J., Tan, F., Feng, X., Zeng, S. The geochemistry of trace elements in marine oil shales and their combustion residues: occurrence and environmental aspects. *Energy Sources A: Recovery Utilization, and Environmental Effects*, 2016b, **38**(3), 410–419. https://doi.org/10.1080/15567036.2013.769036
12. Taylor, S. R., McLennan, S. M. *The Continental Crust: Its Composition and Evolution*. Blackwell Scientific, Oxford, 1985.
13. Taylor, S. R., McLennan, S. M. The geochemical evolution of the continental crust. *Reviews of Geophysics*, 1995, **33**(2), 241–265. https://doi.org/10.1029/95RG00262
14. Patterson, J. H., Ramsden, A. R., Dale, L. S., Fardy, J. J. Geochemistry and mineralogical residences of trace elements in oil shales from Julia Creek, Queensland, Australia. *Chemical Geology*, 1986, **55**(1–2), 1–16. https://doi.org/10.1016/0009-2541(86)90123-3
15. Gao, S., Luo, T.-C., Zhang, B.-R., Zhang, H.-F., Han, Y.-W., Hu, Y.-K. et al. Chemical composition of the continental crust as revealed by studies in East China. *Geochimica et Cosmochimica Acta*, 1998, **62**(11), 1959–1975. https://doi.org/10.1016/S0016-7037(98)00121-5
16. McLennan, S. M. Relationships between the trace element composition of sedimentary rocks and upper continental crust. *Geochemistry, Geophysics, Geosystems*, 2001, **2**(4), 2000GC00010. https://doi.org/10.1029/2000GC000109
17. Rudnick, R., Gao, S. Composition of the Continental Crust. In *Treatise on Geochemistry 3* (Holland, H. D, Turekian, K. K., eds). Elsevier-Pergamon, Oxford, 2003, 1–64.
18. Haskin, L. A., Wildeman, T. R., Haskin, M. A. An accurate procedure for the determination of the rare earths by neutron activation. *Journal of Radioanalytical and Nuclear Chemistry*, 1968, **1**, 337–348. https://doi.org/10.1007/BF02513689
19. Boynton, W. V. Cosmochemistry of the rare earth elements: meteorite studies. In *Rare Earth Element Geochemistry* (Henderson, P., ed.). Elsevier, New York, 1984, 63–114.
20. Gromet, L. P., Haskin, L. A., Korotev, R. L., Dymek, R. F. The "North American shale composite": its compilation, major and trace element characteristics. *Geochimica et Cosmochimica Acta*, 1984, **48**(12), 2469–2482. https://doi.org/10.1016/0016-7037(84)90298-9
21. Wedepohl, K. H. Environmental influences on the chemical composition of shales and clays. *Physics and Chemistry of the Earth*, 1971, **8**, 307–331. https://doi.org/10.1016/0079-1946(71)90020-6
22. Wedepohl, K. H. The composition of the upper Earth's crust and the natural cycles of selected elements. Metals in natural raw materials. Natural resources. In *Metals and Their Compounds in the Environment* (Merian, E., ed.). VCH, Weinheim, 1991, 3–17.
23. Heinrichs, H., Schulz-Dobrick, B., Wedepohl, K. H. Terrestrial geochemistry of Cd, Bi, Tl, Pb, Zn and Rb. *Geochimica et Cosmochimica Acta*, 1980, **44**(10), 1519–1533. https://doi.org/10.1016/0016-7037(80)90116-7
24. Brumsack, H.-J. The trace metal content of recent organic carbon-rich

sediments: implications for Cretaceous black shale formation. *Palaeogeography, Palaeoclimatology, Palaeoecology*, 2006, **232**(2–4), 344–361. https://doi.org/10.1016/j.palaeo.2005.05.011

25. Shpirt, M. Y., Punanova, S. A. Comparative assessment of the trace-element composition of coals, crude oils, and oil shales. *Solid Fuel Chemistry*, 2007, **41**, 267–279. https://doi.org/10.3103/S0361521907050023
26. Ross, D. J. K., Bustin, R. M. Investigating the use of sedimentary geochemical proxies for paleoenvironment interpretation of thermally mature organic-rich strata: examples from the Devonian–Mississippian shales, Western Canadian Sedimentary Basin. *Chemical Geology*, 2009, **260**(1–2), 1–19. https://doi.org/10.1016/j.chemgeo.2008.10.027
27. Jelenković, R., Kostić, A., Životić, D., Ercegovac, M. Mineral resources of Serbia. *Geologica Carpathica*, 2008, **59**(4), 345–361.
28. Obradović, J., Djurdjević-Colson, J., Vasić, N. Phytogenic lacustrine sedimentation – oil shales in Neogene from Serbia, Yugoslavia. *Journal of Paleolimnology*, 1997, **18**, 351–364. https://doi.org/10.1023/A:1007907109399
29. Obradović, J., Vasić, N. *Jezerski baseni u neogenu Srbije (Neogene Lacustrine Basins from Serbia)*. Srpska akademija nauka i umetnosti, Beograd, 2007.
30. Marović, M. Neotektonski sklop Aleksinačkog Pomoravlja (Neotectonic complex of Aleksinac Pomoravlje). *Geološki Anali Balkanskoga Poluostrva*, 1988, **51**, 215–219.
31. Ercegovac, M., Vitorović, D., Kostić, A., Životić, D., Jovančićević, B. Geology and Geochemistry of the "Aleksinac" oil shale deposit (Serbia). In *Joint 61st ICCP/26th TSOP Meeting, Advances in Organic Petrology and Organic Geochemistry*, 19–26 September 2009, Gramado, Brazil, 13.
32. Gajica, G., Šajnović, A., Stojanović, K., Antonijević, M., Aleksić, N., Jovančićević, B. The influence of pyrolysis type on shale oil generation and its composition (Upper layer of Aleksinac oil shale, Serbia). *Journal of the Serbian Chemical Society*, 2017b, **82**(12), 1461–1477. https://doi.org/10.2298/JSC170421064G
33. Gajica, G., Šajnović, A., Stojanović, K., Kostić, A., Slipper, I., Antonijević, M. et al. Organic geochemical study of the Upper layer of Aleksinac oil shale in the Dubrava block, Serbia. *Oil Shale*, 2017, **34**(3), 197–218. https://doi.org/10.3176/oil.2017.3.01
34. Tribovillard, N., Algeo, T. J., Lyons, T., Riboulleau, A. Trace metals as paleoredox and paleoproductivity proxies: an update. *Chemical Geology*, 2006, **232**(1–2), 12–32. https://doi.org/10.1016/j.chemgeo.2006.02.012
35. Ferriday, T., Montenari, M. Chemostratigraphy and chemofacies of source rock analogues: a high-resolution analysis of black shale successions from the lower Silurian Formigoso Formation (Cantabrian Mountains, NW Spain). In *Stratigraphy & Timescales* (Montenari, M., ed.). Elsevier Science, Amsterdam, 2016, 123–255.
36. Mukhopadhyay, P. K., Goodarzi, F., Crandlemire, A. L., Gillis, K. S., MacNeil, D. J., Smith, W. D. Comparison of coal composition and elemental

distribution in selected seams of the Sydney and Stellarton Basins, Nova Scotia, Eastern Canada. *International Journal of Coal Geology*, 1998, **37**(1–2), 113–141. https://doi.org/10.1016/S0166-5162(98)00020-2

37. Fu, X., Wang, J., Zeng, Y., Tan, F., Feng, X. REE geochemistry of marine oil shale from the Changshe Mountain area, northern Tibet, China. *International Journal of Coal Geology*, 2010, **81**(3), 191–199. https://doi.org/10.1016/j.coal.2009.12.006
38. Tao, S., Xu, Y., Tang, D., Xu, H., Li, S., Chen, S. et al. Geochemistry of the Shitoumei oil shale in the Santanghu Basin, Northwest China: implications for paleoclimate conditions, weathering, provenance and tectonic setting. *International Journal of Coal Geology*, 2017, **184**, 42–56. https://doi.org/10.1016/j.coal.2017.11.007
39. Wang, Z., Fu, X., Feng, X., Song, C., Wang, D., Chen, W. et al. Geochemical features of the black shales from the Wuyu Basin, southern Tibet: implications for palaeoenvironment and palaeoclimate. *Geological Journal*, 2017, **52**(2), 282–297. https://doi.org/10.1002/gj.2756
40. Zhao, M., Liu, Y., Jiao, X., Zhou, D., Meng, Z., Yang, Y. Major, trace and rare earth element geochemistry of the Permian Lucaogou oil shales, eastern Junggar Basin, NW China: implications for weathering, provenance and tectonic setting. *Australian Journal of Earth Sciences*, 2023, **70**(4), 585–602. https://doi.org/10.1080/08120099.2023.2186951
41. Wu, C., Tuo, J., Zhang, M., Liu, Y., Xing, L., Gong, J. et al. Multiple controlling factors of lower Palaeozoic organic-rich marine shales in the Sichuan Basin, China: evidence from minerals and trace elements. *Energy Exploration & Exploitation*, 2017, **35**(5), 627–644. https://doi.org/10.1177/0144598717709667
42. Liang, Y., Zhang, J., Liu, Y., Tang, X., Li, Z., Ding, J. et al. Evidence for biogenic silica occurrence in the Lower Silurian Longmaxi shale in southeastern Chongqing, China. *Minerals*, 2020, **10**(11), 945. https://doi.org/10.3390/min10110945
43. Pipe, A. B., Leybourne, M. I., Johannesson, K. H., Hannigan, R. E., Layton-Matthews, D. Trace and rare earth element geochemistry of black shales from the Upper Ordovician Utica Shale magnafacies. *Chemical Geology*, 2025, **672**, 122507. https://doi.org/10.1016/j.chemgeo.2024.122507
44. Dar, S. A., Khan, K. F., Birch, W. D. Sedimentary: phosphates. In *Reference Module in Earth Systems and Environmental Sciences* (Elias, S. A., ed.). Elsevier, 2017.
45. Wall, F. Rare earth elements. In *Encyclopedia of Geology, 2nd ed.* (Alderton, D., Elias, S. A., eds). Academic Press, London, 2021, 680–693.
46. Al-Ayed, O. S., Qawaqneh, M. K., Abu-Nameh, E. S. M. Tracing rare earth elements in oil shale ash. *Oil Shale*, 2024, **41**(2), 132–143. https://doi.org/10.3176/oil.2024.2.04
47. Algeo, T. J., Tribovillard, N. Environmental analysis of paleoceanographic systems based on molybdenum–uranium covariation. *Chemical Geology*, 2009, **268**(3–4), 211–225. https://doi.org/10.1016/j.chemgeo.2009.09.001